

PACS numbers: 42.55.Ks; 42.60.Lh
DOI: 10.1070/QE2001v031n04ABEH001936

A 400-W repetitively pulsed DF laser

Yu N Aksenov, V P Borisov, Val V Burtsev, S D Velikanov, S L Voronov, V V Voronin, A F Zapol'skii, G A Kirillov, O I Kovalenko, V I Lazarenko, V M Mis'ko, V M Murugov, V D Selemir, S N Sin'kov, Yu N Frolov, V P Tsiberev, Yu N Sheremet'ev

***Abstract*. Results of a study of a repetitively pulsed three-module electric-discharge DF laser operating on an $SF_6 - D_2$ mixture are reported. It is shown that the optimisation of the cavity *Q*-factor, the pressure of the working mixture, and its composition, provides a 400-W output power at a pulse repetition rate of ~ 10 Hz.**

Keywords: *repetitively pulsed regime, electric-discharge laser, DF laser.*

1. Introduction

The main problem of laser ecological monitoring of the atmosphere consists in determining concentrations of gases and different aerosols at a large distance from a radiation source. One of the most interesting spectral regions from the viewpoint of the presence of absorption bands is the region between 3 and 5 μm. Because of this, repetitively pulsed DF lasers ($\lambda = 3.5 - 4.0$ μm) based on the chain reaction of fluorine with chlorine and using a closed circulation of the active medium is a promising radiation source for lidars.

The use of such lasers offers the following metrological and operating advantages in lidar systems:

(1) The possibility of laser operation in a repetitive pulsed regime, which provides a rapid localisation of gaseous and aerosol impurities when scanning a laser beam in space;

(2) the stability of output laser parameters, the reliability and the ecological safety of laser operation because of an absolute chemical stability of working mixtures and the closed cycle of their replacement.

The emission spectrum of a DF laser consists of several dozens of lines. The relative portion of the energy emitted in separate spectral lines ranges from ~ 1 % to ~ 10 % [2].

Yu N Aksenov, V P Borisov, Val V Burtsev, S D Velikanov, S L Voronov, V V Voronin, A F Zapol'skii, G A Kirillov, O I Kovalenko, V I Lazarenko, V M Mis'ko, V M Murugov, V D Selemir, S N Sin'kov, Yu N Frolov, V P Tsiberev, Yu N Sheremet'ev All-Russian Research Institute of Experimental Physics, All-Russian Federal Nuclear Centre, prosp.Mira 37, 607190 Sarov, Nizhegorodskaya oblast, Russia;
e-mail: velikanov@otd 13.vnief.ru

Received 14 September 2000
Kvantovaya Elektronika **31** (4) 290 – 292 (2001)
Translated by A N Kirkin

The possibility of using this laser for the remote analysis of gas impurities in the atmosphere was demonstrated in studies [3 – 6]. As shown in Ref. [4], using a DF laser, one can reliably measure the concentration of such impurities as gaseous hydrocarbons, HCl, N_2O, and SO_2. It follows from the calculation of the lidar signal that the signal-to-noise ratio for probing radiation with an energy of ~ 1 J, the receiving telescope with an area of ~ 1 m^2, a detector sensitivity of $\sim 5 \times 10^{-10}$ W Hz$^{-1/2}$ cm^{-1}, and a distance to an aerosol or a gaseous cloud of about a few kilometers can reach 100. To obtain the emission energy ~ 1 J, in a separate line, the total output laser energy integrated over the spectrum should be as high as dozens of Joules.

In this paper, we analyse the possibility of obtaining the output energy of a repetitively pulsed DF laser as high as several dozens of Joules.

2. Experimental

In Ref. [7], we presented the results of our study of an electric-discharge DF laser producing single pulses. We found that the output radiation energy of the laser with the optimised composition of the working mixture, its pressure, and reflectivity of the output cavity mirror reached ~ 10 J. One of the ways of increasing the laser energy is to use several electric-discharge laser modules of the same type, which are aligned along one optical axis [8].

These modules are powered from a sectionalised power supply with a common synchronisation system. In this work, we used three laser modules with identical discharge formation systems, which are described in Ref. [7]. The synchronisation system provided the supply of voltage to the electrodes of the system with a jitter of ± 20 ns and, therefore, a simultaneous formation of the volume discharge in all laser modules.

The replacement of the working $SF_6 - D_2$ mixture in the discharge volume was provided by gas circulation in a closed circuit with the aid of fans [1]. The gas flow passed through the electrodes (the flow velocity vector was perpendicular to the electrode plane), and its velocity in the discharge volume was $\sim 3 - 4$ m s^{-1}.

Fig. 1 presents the optical schematic of the experiments. The laser cavity was formed by a plane mirror *3* with the reflectivity 99 % and a plane output mirror *4* with the reflectivity from 5.6 % to 36 %. Windows *2* of a working laser chamber *1* were aligned parallel to the cavity mirrors. A spherical mirror *10* with the focal distance $F = 1000$ mm and a lens *11* with $F = 670$ mm focused laser radiation onto TPI-E calorimeters *13*. A lens *12* with $F = 1000$ mm focused

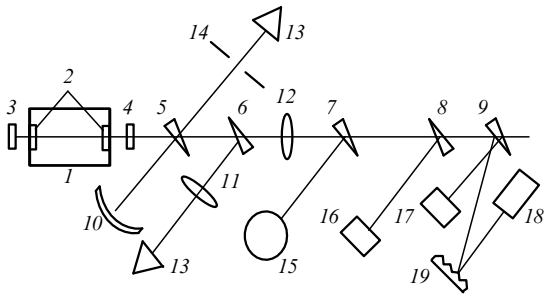

Figure 1. Optical schematic of the experimental setup: (*1*) DF laser; (*2*) windows of the working chamber; (*3*) plane mirror with reflectivity $\sim 99\,\%$; (*4*) plane output mirror; (*5–9*) wedge-like beamsplitters; (*10*) spherical mirror with $F = 1000$ mm; (*11*) CaF_2 lens with $F = 670$ mm; (*12*) CaF_2 lens with $F = 1000$ mm; (*13*) TPI-E calorimeter; (*14*) aperture; (*15*) rotating cylinder; (*16*) recorder of laser radiation in the near-field zone; (*17*) recorder of the laser pulse shape; (*18*) RjP-735 radiometer; (*19*) diffusely scattering aluminium screen.

radiation onto a set of detectors: a rotating cylinder *15*, which provided recording of the near-field zone image of a laser beam on a thermosensitive screen; a recorder of laser radiation in the near-field region on a thermophotographic film [9]; a semiconductor ionisation chamber *17* [10] recording the laser pulse shape; and an RjP-735 radiometer *18* for measuring the radiation energy in each pulse.

3. Experimental results and their discussion

At the first stage of experiments, we studied characteristics of the laser operating in the single-pulse mode. The experiments were carried out for the $SF_6 : D_2 = 10 : 1$ mixture, with the total pressure p varied in the range from 0.08 to 0.12 at. Figs 2 and 3 present the dependences of the output laser energy E_{out} on the reflectivity of the output cavity mirror R_{out} for $p = 0.10$ at and on the pressure of the working mixture for different R_{out}. The maximum laser power of ~ 40 J was obtained for $R_{out} = 16\,\%$ and $p = 0.10$ at.

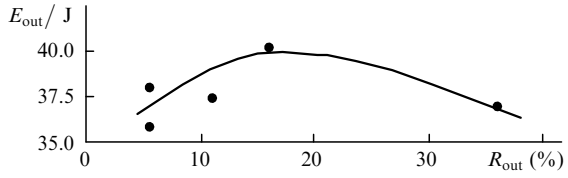

Figure 2. Dependence of the output laser energy E_{out} on the reflectivity R_{out} of the output cavity mirror for the working-mixture pressure p = 0.10 at.

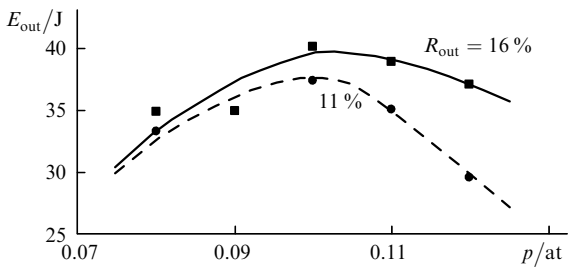

Figure 3. Dependences of the output laser energy E_{out} on the mixture pressure p for different reflectivities R_{out} of the output cavity mirror.

The analysis of the results obtained shows that the increase in the length of the active medium by a factor of three compare to the laser described in Ref. [7] caused a change in the optimum reflectivity of the output cavity mirror from ~ 36 to $\sim 16\,\%$ and an increase in the output energy (per laser module) from ~ 10.5 to ~ 13.3 J. These results are adequately described by an increase in the length of the active medium and the specific input electric energy. The technical laser efficiency under optimum operating conditions was $\eta_t = E_{out}/E_0 \approx 2.3\%$ (E_0 is the stored electric energy), which agrees well with the value reported in Ref. [7].

In a series of experiments, laser radiation in the near-field zone was recorded on a thermophotographic film. The spatial resolution of the recording system in the image plane was estimated as 0.5 lines mm^{-1}. The image obtained in the near-field zone in one of the experiments and results of its processing are presented in Figs 4 and 5.

The preliminary analysis of the results of processing the near-field zone image showed that the radiation beam in the near-field zone was virtually rectangular in shape, with a horizontal size of 120 mm (the interelectrode spacing) and

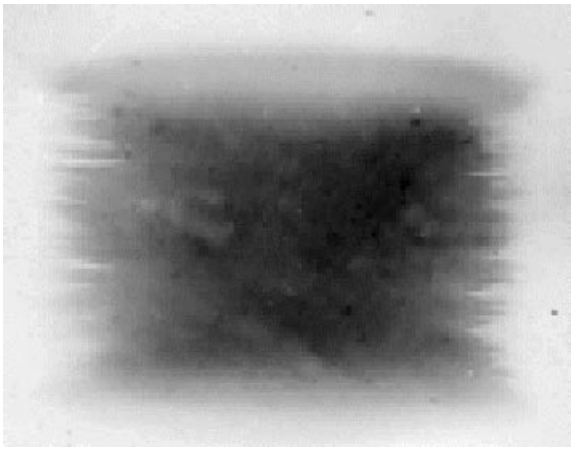

Figure 4. Near-field zone of laser emission.

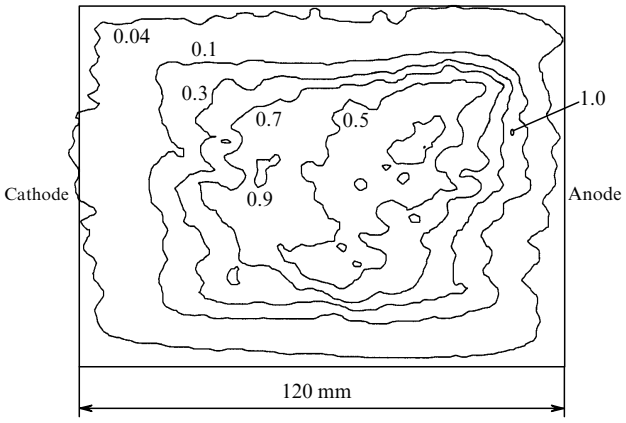

Figure 5. Isolines of the relative density of laser energy in the near-field zone.

avertical size of ~ 100 mm. From this it follows that we had the active laser volume $V_a = 10.8$ litre and the average specific output energy $\varepsilon \approx 3.7$ J litre^{-1}. The images manifested a sharp decrease in the output-energy density in the regions 10–14 mm wide at all the edges of the active medium. According to our estimates, the edges occupy approximately 37 % of the volume of the active medium, i.e., 4 litre, and the average specific output energy there is only ~ 0.7 J litre^{-1}. The cross section of the lasing region has the shape of a rectangle with horizontal and vertical dimensions of ~ 94 and ~ 78 mm, respectively. Its volume is approximately 63 % of the total volume of the active medium, i.e., 6.8 litre. In this region, $\varepsilon \approx 5.5$ J litre^{-1}, with the maximum local specific output energy ε_{max} reaching ~ 11 J litre^{-1}. The presence of near-electrode regions with a low emission energy (especially near the cathode) can be attributed to a partial shading of laser emission by the plasma of unfinished streamers and strong nonuniformities of the energy deposition.

In the experiments, we measured parameters of the electric discharge in the working chamber. Fig. 6 presents typical oscillograms of voltage across the electrodes and discharge current for the stored electric energy $E_0 \approx 1700$ J, the pressure of the working medium $p = 0.10$ at, and its composition $SF_6 : D_2 = 10 : 1$.

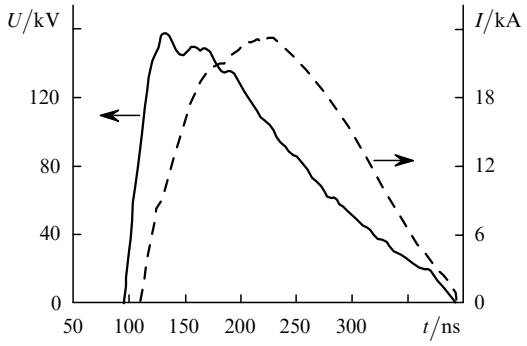

Figure 6. Oscillograms of voltage across the electrodes and discharge current.

One can see from Fig. 6 that the voltage on each of the electrodes relative to the ground reached approximately ± 160 kV and the discharge current reached ~ 23 kA (in one laser module). The calculated time dependences (obtained from the experimentally recorded oscillograms of voltage and current pulses) of the deposited electric energy and the discharge resistance are presented in Fig. 7. It follows from Figs 6 and 7 that the duration of the initiating pulse (the current pulse) was $\tau \approx 270 \pm 30$ ns and the total electric energy deposited into the discharge in three modules was ~ 1200 J, which is about 70 % of the energy stored in the energy supply.

At the second stage of experiments, we studied lasing in the repetitively pulsed regime. A typical duration of laser operation with the pulse repetition rate $f \sim 10$ Hz (10–13 pulse in a series) was about 0.8–1.3 s. In these experiments, we also measured the total energy of laser pulses in a series by a TPI-E calorimeter and the energy of each pulse in a series by an RjP-735 calorimeter. The output data were entered into a computer.

The average energy of laser pulses in different series was $\bar{E}_{out} \approx 34 - 35$ J, with the mean-square deviation $\delta \approx 0.3$–1 J. The average output laser energy was ~ 400 W.

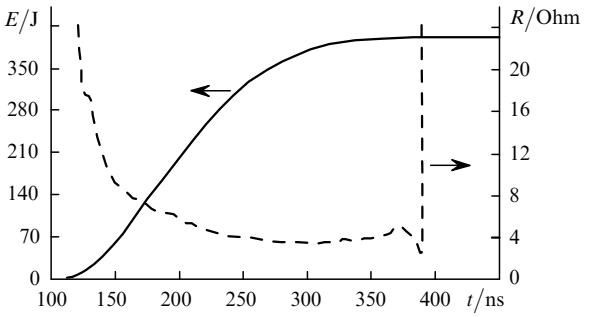

Figure 7. Time dependences of the deposited electric energy E and the discharge resistance R for one of the modules.

Estimates of the technical laser efficiency in the repetitively pulse regime give $\eta_t \approx 2 - 2.1\%$, which is approximately 0.9 of the technical efficiency obtained in the pulsed regime. It is likely that the difference is caused by an increase in the discharge streaming probability.

The results obtained show that the repetitively pulsed DF laser that was experimentally studied in this work can be used for atmospheric monitoring.

References

1. Velikanov S D, Zapol'skii A F, Frolov Yu N *Kvantovaya Elektron.* **24** 11 (1997) [*Quantum Electron.* **27** 9 (1997)]
2. Spencer D J, Denault G C, Takimoto H H *Appl. Opt.* **13** 2855 (1974)
3. Murray E R, van der Laan J E, Hawley J G *Appl. Opt.* **15** 3140 (1976)
4. Velikanov S D, Elutin A S, Kudryashov E A, Peroev I N, Sin'kov S N, Frolov Yu N *Kvantovaya Elektron.* **24** 279 (1997) [*Quantum Electron.* **27** 273 (1997)]
5. Velikanov S D, Elutin A S, Pegoev I N, Sin'kov S N, Frolov Yu N *Kvantovaya Elektron.* **25** 181 (1998) [*Quantum Electron.* **28** 171 (1998)]
6. O'Connor S J, Walnslay H L, Pasley J G *Proc. SPIE Int. Soc. Opt. Eng.* **3493** 255 (1998)
7. Borisov V P, Burtsev Val V, Velikanov S D, Voronov S L, Voronin V V, Zapol'skii A F, Zolotov M I, Kirillov G A, Mishchenko G M, Podavalov A M, Selemir V D, Urlin V D, Frolov Yu N, Tsiberov V P *Kvantovaya Elektron.* **30** 225 (2000) [*Quantum Electron.* **30** 225 (2000)]
8. Kudryashov V P, Osipov V V, Sanin V V *Kvantovaya Elektron.* **6** 417 (1979) [*Quantum Electron.* **9** 254 (1979)]
9. Astrov Yu A, Egorov V V, Murugov V M, Sheremet'ev Yu N *Kvantovaya Electron.* **4** 1681 (1977) [*Quantum Electron.* **7** 954 (1977)]
10. Kovalev V I, Leciv A R, Faizullin F S, Fedorov B F *Prib. Tekh. Eksp.* (1) 149 (1983)